Hindawi
Journal of Nanomaterials
Volume 2019, Article ID 8293427, 11 pages
https://doi.org/10.1155/2019/8293427

Research Article

Anodic Growth Behavior of TiO_2 Nanotube Arrays with Process Parameter Control

Wan-Tae Kim[1] **and Won-Youl Choi**[1,2]

[1]*Department of Advanced Materials Engineering, Gangneung-Wonju National University, Gangneung, Gangwon 25457, Republic of Korea*
[2]*Research Institute for Dental Engineering, Gangneung-Wonju National University, Gangneung, Gangwon 25457, Republic of Korea*

Correspondence should be addressed to Won-Youl Choi; cwy@gwnu.ac.kr

Received 23 May 2018; Accepted 3 October 2018; Published 18 February 2019

Academic Editor: Nageh K. Allam

TiO_2 nanotube arrays are very attractive materials by their vertically aligned porous nanostructures. They are easy to make using an anodic oxidation process in organic and inorganic electrolytes containing halogen ions, like fluorine and chlorine. Their growth tendency, various microstructures of TiO_2 nanotube arrays, was fabricated and analysed with controlling of anodic oxidation process parameter like applied voltage, process time, electrolyte temperature, concentration of ammonium fluoride and DI water in ethylene glycol electrolyte, voltage applying and dropping rate, grain orientation, and size of titanium foil. Pore diameter and length were controlled in the range of 16 nm to 178 nm and 0.2 μm to 14.6 μm, respectively. Some tendencies of their growth were observed with different anodic oxidation variables. This growth tendency of TiO_2 nanotube arrays is should be considered before they used in many applications, and if optimal structure for each application was fabricated and used, they will show better performance.

1. Introduction

Titanium dioxide has excellent chemical, electrical, and optical properties and chemical stability. For that reason, it is used in many different fields of study and industry, such as dye-sensitized solar cells [1–3], perovskite sensitized solar cells [4–6], photocatalysts [7], metal oxide semiconductor gas sensors [8, 9], dental implants [10, 11], interferometric sensors [12, 13], photonic crystals [14], and other applications. Typically, it is very useful materials for electron transport materials of organic solar cells due to their electronic band gap, nontoxic properties, and low product cost. Many nanostructures of TiO_2 reported to improve their specific area and electron-hole recombination, like nanoparticles [1, 3, 15], nanofibers [16, 17], and nanotubes [7, 8, 10, 12, 13, 18–20]. One of them, TiO_2 nanotube arrays are very attractive materials for higher electron transport materials by their vertically aligned porous nanostructures. Also, they have large specific surface area, open window, and excellent chemical and mechanical properties, and it have extended the application fields to photoanode of organic solar cells and others. TiO_2 nanotube arrays are easy to make using an anodic oxidation process in organic and inorganic electrolytes containing halogen ions, like fluorine and chlorine. The fabrication of TiO_2 nanotube arrays via anodic oxidation of titanium foil in fluoride-based solution was first reported in 2003 by Beranek et al. [21]. In anodic oxidation, dissolution and oxidation are very important as formation mechanism, and they are affected by process parameter such as chemical composition of electrolyte, applied voltage, processing time, and temperature. Organics or aqueous solutions have been used as an electrolyte, and they contain fluorine-based materials, such as hydrogen fluoride, potassium fluoride, and ammonium fluoride [18–20, 22]. The voltage of 10 to 60 V is usually

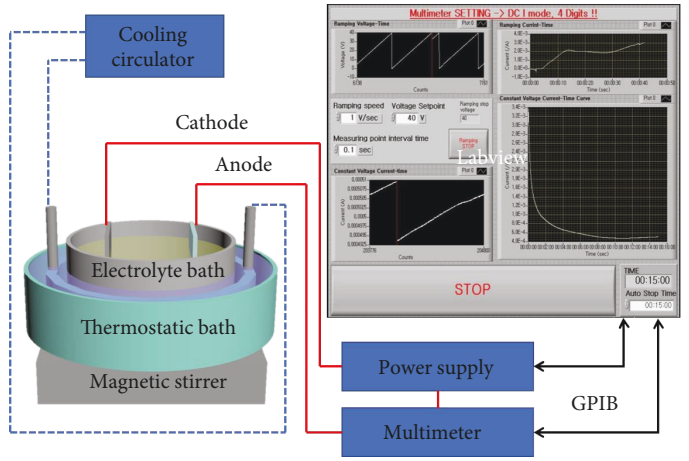

Figure 1: Schematic diagram of potentiostatic electrochemical system.

Table 1: Anodic oxidation conditions of different process time, electrolyte temperature, and concentration of NH_4F and DI water in ethylene glycol electrolyte.

Control parameter	Voltage (V)	Time (minute)	NH_4F (wt%)	DI water (vol%)	Temperature (°C)
Process time	60	*10*	0.5	2.2	30
	60	*20*	0.5	2.2	30
	60	*30*	0.5	2.2	30
	60	*40*	0.5	2.2	30
	60	*50*	0.5	2.2	30
	60	*60*	0.5	2.2	30
Temperature	60	360	0.5	10.9	*0*
	60	360	0.5	10.9	*15*
	60	360	0.5	10.9	*30*
Concentration of NH_4F	60	360	*0.3*	10.9	30
	60	360	*0.5*	10.9	30
	60	360	*1.0*	10.9	30
Concentration of DI water	60	30	0.5	*2.2*	30
	60	30	0.5	*5.3*	30
	60	30	0.5	*10.9*	30

Table 2: Anodic oxidation conditions of different voltage applying rate and dropping rate.

Control parameter	Applying speed (V/s)	Dropping speed (V/s)
Applying speed control	*0.1*	Immediately dropped
	0.5	Immediately dropped
	5.0	Immediately dropped
	10.0	Immediately dropped
	30.0	Immediately dropped
	60.0	Immediately dropped
	1.0	Immediately dropped
Dropping speed control	1.0	*1.0*
	1.0	*0.1*

applied, and variable voltage steps are also conducted. Processing time is very diverse according to other conditions. To apply for various application fields, a suitable microstructure for the nanotube diameter, the nanotube length, and the surface state is needed and fabricated.

In this study, to understand their growth tendency, various microstructures of TiO_2 nanotube arrays were fabricated and analysed with controlling of anodic oxidation process parameter like applied voltage, process time, electrolyte temperature, concentration of ammonium fluoride and DI water in ethylene glycol electrolyte, voltage applying and dropping rate, grain orientation, and size of titanium foil. And their pore diameter and pore length are measured and observed by field emission scanning electron microscope (FE-SEM, FEI Co., Inspect F/Hitachi Ltd., SU-70). Some tendencies of their growth were observed with different anodic oxidation variables.

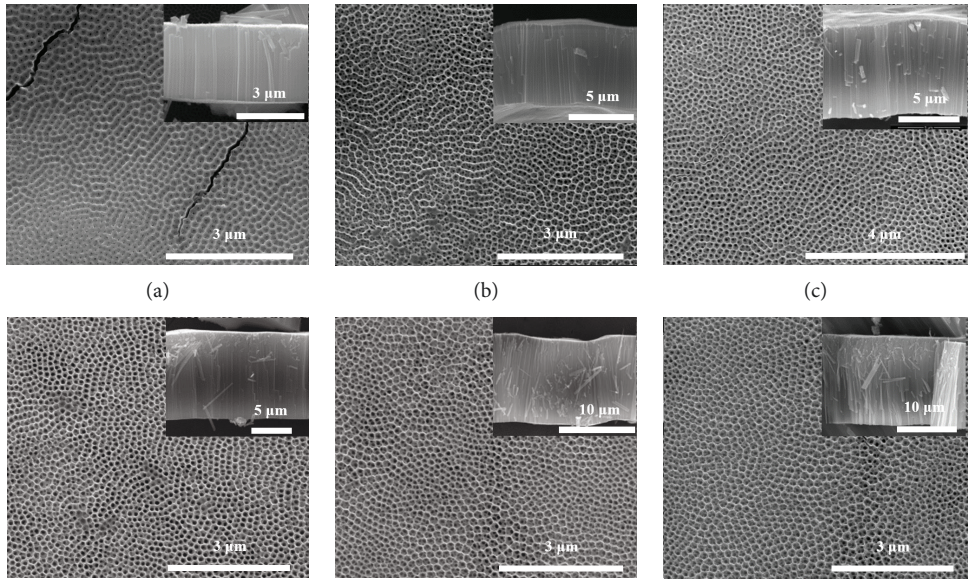

Figure 2: FE-SEM image of TiO_2 nanotube arrays with different process time ((a) 10 min, (b) 20 min, (c) 30 min, (d) 40 min, (e) 50 min, and (f) 60 min).

2. Materials and Methods

Figure 1 shows potentiostatic electrochemical system. The system consisted of a power supply (Xantrex Co., XKW 600), multimeter (Agilent Co., 34401A), constant temperature water bath, and PC. The power supply and multimeter were computer-controlled by the LabVIEW (National Instruments Co.) program for electropolishing and anodic oxidation.

To compare the microstructure with different process time, electrolyte temperature, and concentration of ammonium fluoride (NH_4F, JUNSEI Co.) and DI water in ethylene glycol (JUNSEI Co.) electrolyte, titanium foils (Alfa Aesar Co., 0.89 mm thickness, 99.7% purity) were rinsed in an ultrasonic bath of DI water, ethyl alcohol, and acetone for 10 min in turn and dried at room temperature in a convection oven to remove the surface pollutant. And Ti foil was anodic oxidized in each condition, which is shown in Table 1. For the comparison of microstructure after anodic oxidation, process time, temperature, and concentration of NH_4F and DI water were controlled in a range of 10 ~ 60 min, 0 ~ 30°C, 0.3 ~ 1.0 wt%, and 2.2 ~ 10.9 vol%, respectively. Other conditions of anodic oxidation were the same for each comparison.

Secondly, some titanium foil was conducted in anodic oxidation process for different applied voltage, voltage applying rate, and dropping rate. Applied voltage was controlled in a range of 3 ~ 60 V at 30°C for 4 hr in ethylene glycol electrolyte with 0.5 wt% NH_4F and 10.9 vol% DI water; Table 2 shows voltage applying rate and dropping rate conditions, and they are controlled in a range of 0.1 ~ 60.0 V/s, immediately drop ~0.1 V/s anodic oxidized at 60 V and 30°C for 10 min in ethylene glycol electrolyte with 0.5 wt% NH_4F and 2.2 vol% DI water.

To compare the microstructure with different grain size and orientation, Ti foil was annealed in an electric furnace for 1 hr at 500, 800, 950, and 1100°C. After annealing, to observe the grain size and orientation, Ti foils were mechanically polished by sand paper and were electropolished for 20 V and 5 min in methyl alcohol (J.T.Baker. Co.) with 38 wt% ethylene glycol and 10 wt% perchloric acid (JUNSEI Co., 70%) at 0°C and stirred at 800 rpm. Then, polished titanium foils were etched for 20 sec in DI water with 10 vol% nitric acid and 10 vol% hydrofluoric acid. Grain structure and orientation of etched titanium foils were observed by FE-SEM and X-ray diffractometer (Rigaku D/MAX-RC, Cu Kα radiation). After electropolishing, titanium foils were anodized at 60 V and 30°C for 40 min in ethylene glycol electrolyte with 0.5 wt% NH_4F and 8.2 vol% DI water. Also, after anodic oxidation process, all anodic oxidized samples were immersed in ethyl alcohol and dried in a dry oven. Then, their microstructures were observed by FE-SEM.

3. Results and Discussion

The various microstructures of TiO_2 nanotube arrays were obtained with anodic oxidation process time from 10 min to 60 min at 60 V and 30°C in ethylene glycol electrolyte with 0.5 wt% NH_4F and 2.2 vol% DI water. Figures 2 and 3 show FE-SEM image and their microstructure change of anodic-oxidized TiO_2 nanotube arrays with different process time. With the increase of process time, higher pore diameter and pore length were observed. The pore diameter and pore length of 10 min anodic-oxidized TiO_2 nanotube arrays were 46 nm and 3.4 μm, and the pore diameter and pore length of 60 min anodic-oxidized TiO_2 nanotube arrays were 90 nm and 14.6 μm, respectively.

Figure 4 shows FE-SEM image and their microstructure change of anodic-oxidized TiO_2 nanotube arrays with different electrolyte temperature. Titanium foils were conducted for different electrolyte temperature from 0°C to 30°C at

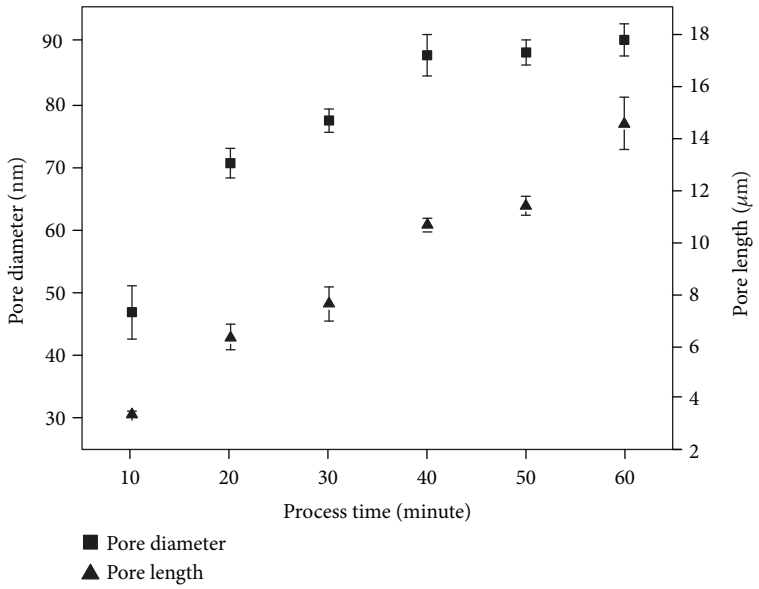

Figure 3: Pore diameter and pore length of TiO_2 nanotube arrays with different process time.

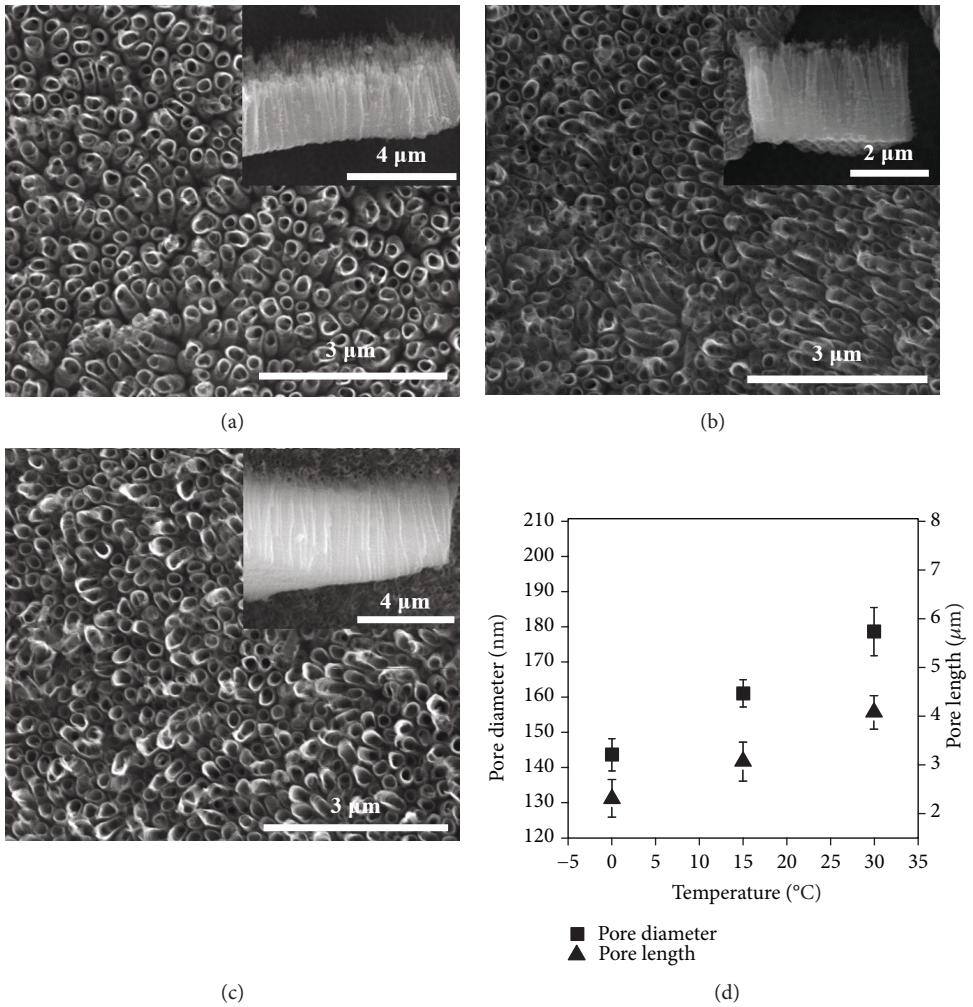

Figure 4: FE-SEM image of TiO_2 nanotube arrays with different electrolyte temperature ((a) 0°C, (b) 15°C, and (c) 30°C) and their microstructure change (d).

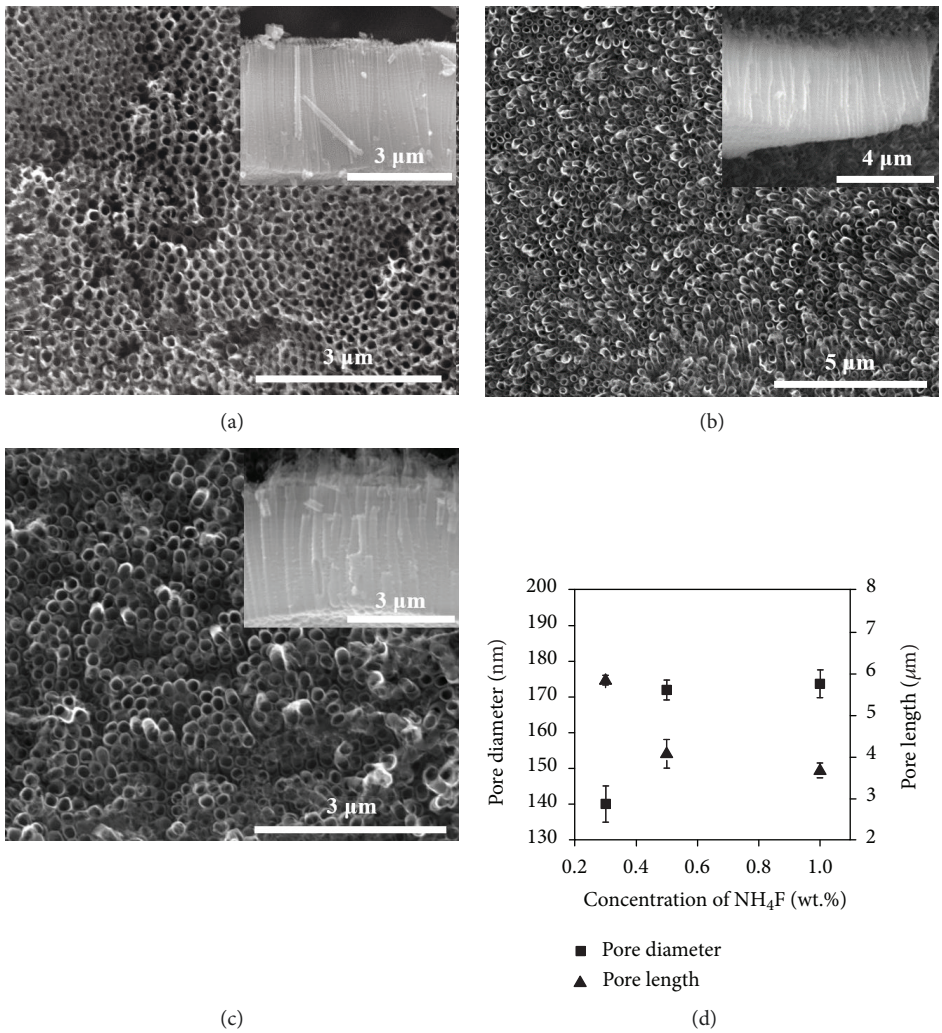

Figure 5: FE-SEM image of TiO_2 nanotube arrays with different concentration of NH_4F in electrolyte ((a) 0.3 wt%, (b) 0.5 wt%, and (c) 1.0 wt%) and their microstructure change (d).

60 V for 4 hr in ethylene glycol electrolyte with 0.5 wt% NH_4F and 10.9 vol% DI water. With the increase of electrolyte temperature, both pore diameter and pore length were increased. The pore diameter and pore length of TiO_2 nanotube arrays which were formed at 0°C were 143 nm and 2.3 μm, respectively, and the pore diameter and pore length of TiO_2 nanotube arrays which were formed at 30°C were 178 nm and 4.1 μm, respectively. It resulted from higher ion diffusivity in higher temperature of electrolyte.

Figure 5 shows FE-SEM image and their microstructure change of anodic-oxidized TiO_2 nanotube arrays with different concentration of NH_4F in electrolyte. For the comparison with different concentration of NH_4F, titanium foils were conducted at 60 V and 30°C for 4 hr in ethylene glycol electrolyte with 0.3 ~ 1.0 wt% NH_4F and 10.9 vol% DI water. With the increase of concentration of NH_4F in electrolyte, pore diameter was increased but pore length was decreased. The pore diameter and pore length of TiO_2 nanotube arrays which were formed in 0.3 wt% NH_4F-contained electrolyte were 140 nm and 5.8 μm, respectively, and the pore diameter and pore length of TiO_2 nanotube arrays which were formed in 1.0 wt% NH_4F-contained electrolyte were 174 nm and 3.7 μm, respectively. NH_4F in electrolyte acted as an etchant for TiO_2 nanotubes during anodic oxidation, and the pores were widened and shortened.

Figure 6 shows FE-SEM image and their microstructure change of anodic-oxidized TiO_2 nanotube arrays with different concentration of DI water in electrolyte. For the comparison with different concentration of DI water, titanium foils were conducted at 60 V and 30°C for 30 min in ethylene glycol electrolyte with 0.5 wt% NH_4F and 2.2 ~ 10.9 vol% DI water. With the increase of concentration of DI water in electrolyte, pore diameter was increased but pore length was decreased. The pore diameter and pore length of TiO_2 nanotube arrays which were formed in 2.2 vol% DI water-contained electrolyte were 72 nm and 7.6 μm, respectively, and the pore diameter and pore length of TiO_2 nanotube arrays which were formed in 10.9 wt% NH_4F-contained electrolyte were 104 nm and 1.0 μm, respectively. Pore length formed in aqueous electrolyte is shorter than that in organic

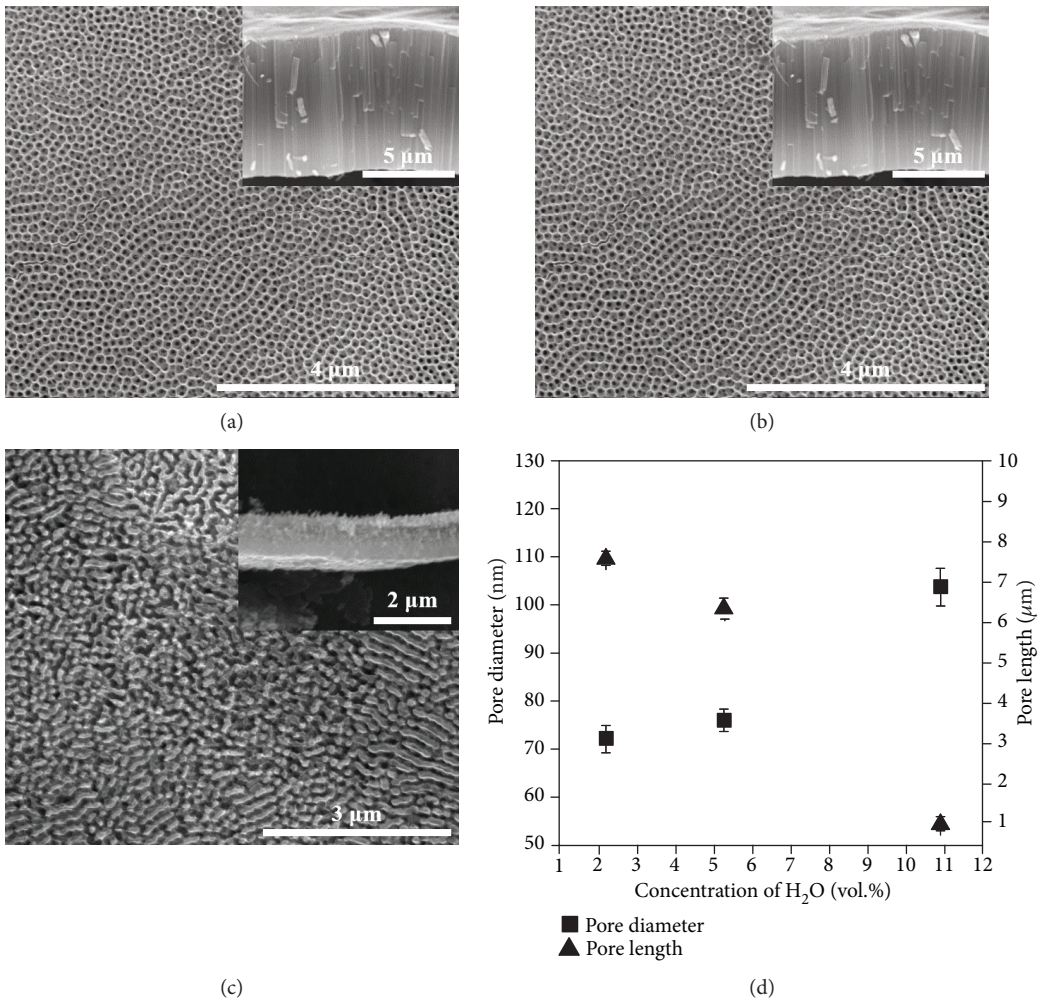

Figure 6: FE-SEM image of TiO_2 nanotube arrays with different concentration of DI water in electrolyte ((a) 2.2 vol%, (b) 5.3 vol%, and (c) 10.9 vol%) and their microstructure change (d).

electrolytes such as ethylene glycol and glycerol [23–25]. The DI water increased the effect of aqueous electrolyte, and the pore length was decreased with DI water.

With 3 V to 60 V range of applied voltage, various microstructures of TiO_2 nanotube arrays were obtained for 4 hr and 30°C in ethylene glycol electrolyte with 0.5 wt% NH_4F and 10.9 vol% DI water. Figures 7 and 8 show FE-SEM image and their microstructure change of anodic-oxidized TiO_2 nanotube arrays with different applied voltage. With the increase of applied voltage, higher pore diameter and pore length were observed. The pore diameter and pore length of TiO_2 nanotube arrays which were fabricated at 60 V were 178 nm and 4.07 μm, respectively, and the pore diameter and pore length of TiO_2 nanotube arrays which were fabricated at 3 V were 16 nm and 0.2 μm, respectively.

Figures 9 and 10 show FE-SEM image and microstructure of anodic-oxidized TiO_2 nanotube arrays with different voltage applying rate and dropping rate. For the comparison with different concentration of DI water, titanium foils were conducted at 60 V and 30°C for 10 min in ethylene glycol electrolyte with 0.5 wt% NH_4F and 2.2 vol% DI water. At 0.5 V/s ~ 30.0 V/s applying rate, there was no obvious difference or slightly changed in pore diameter and pore length, but lower pore diameter and higher pore length were observed at V/s applying rate, and higher pore diameter and lower pore length were observed at 60 V/s applying rate. With the increase of dropping speed, lower pore diameter and pore length were observed. The pore diameter and pore length of TiO_2 nanotube arrays fabricated at 0.5 V/s applying rate were 59 nm and 1.1 μm, respectively. And the pore diameter and pore length of TiO_2 nanotube arrays fabricated at 30.0 V/s applying rate were 83 nm and 1.1 μm, respectively. Also, 73 nm, 1.1 μm and 82 nm, 1.7 μm of pore diameter and pore length were observed, respectively, at 1.0 V/s applying rate, immediately dropped and 1.0 V/s applying rate, 0.1 V/s dropping rate.

Figures 11 and 12 show grain structure, their size, and crystal orientation. To compare with different grain size, orientation, and their anodic oxidation behavior, titanium foil was annealed in an electric furnace for 1 hr at 500, 800, 950, and 1100°C. With the increase of annealing temperature, grain size was increased and their orientation aligned for (110), (012), and (013) plane of α-Ti. Also, each titanium foils were anodic oxidized at 60 V and 30°C for 40 min in ethylene

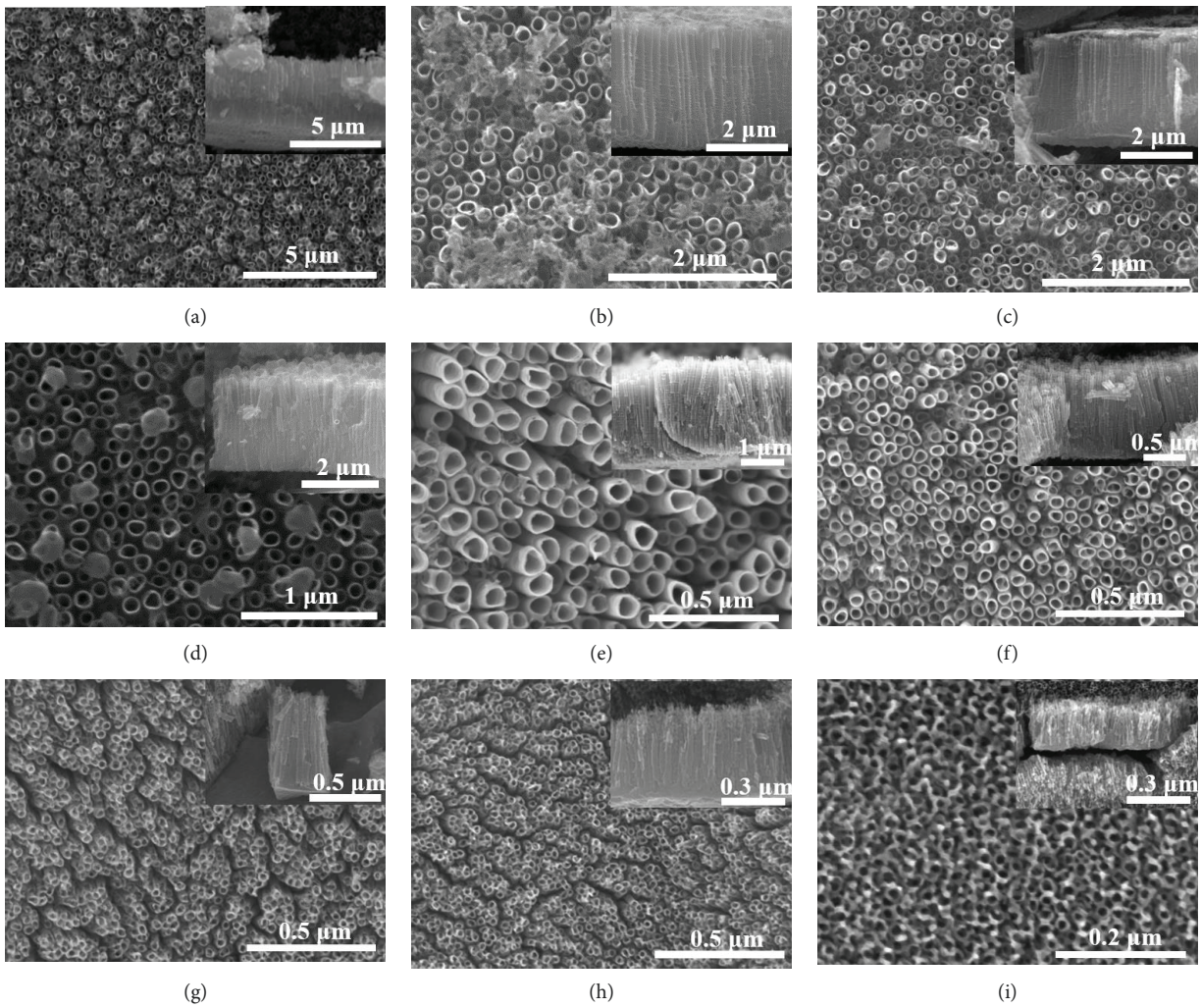

Figure 7: FE-SEM image of TiO_2 nanotube arrays with different applied voltage ((a) 60 V, (b) 50 V, (c) 40 V, (d) 30 V, (e) 20 V, (f) 10 V, (g) 7 V, (h) 5 V, and (i) 3 V).

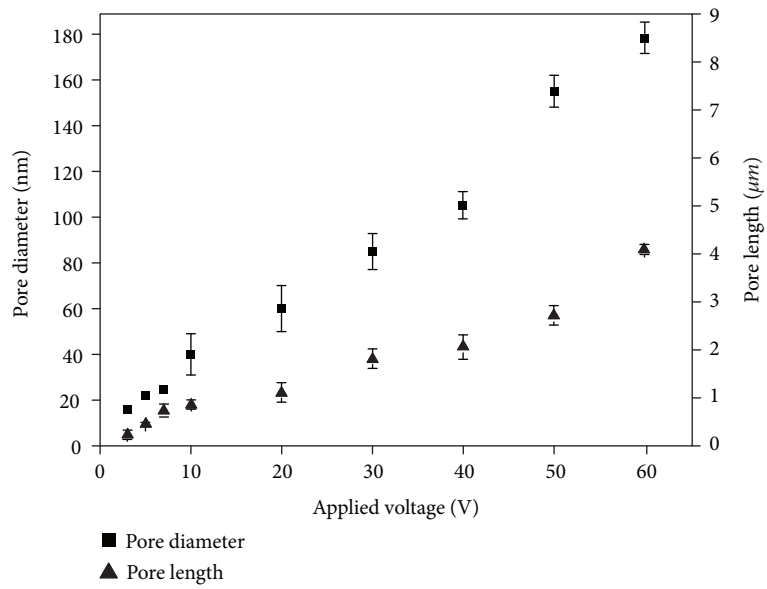

Figure 8: Pore diameter and pore length of TiO_2 nanotube arrays with different applied voltage.

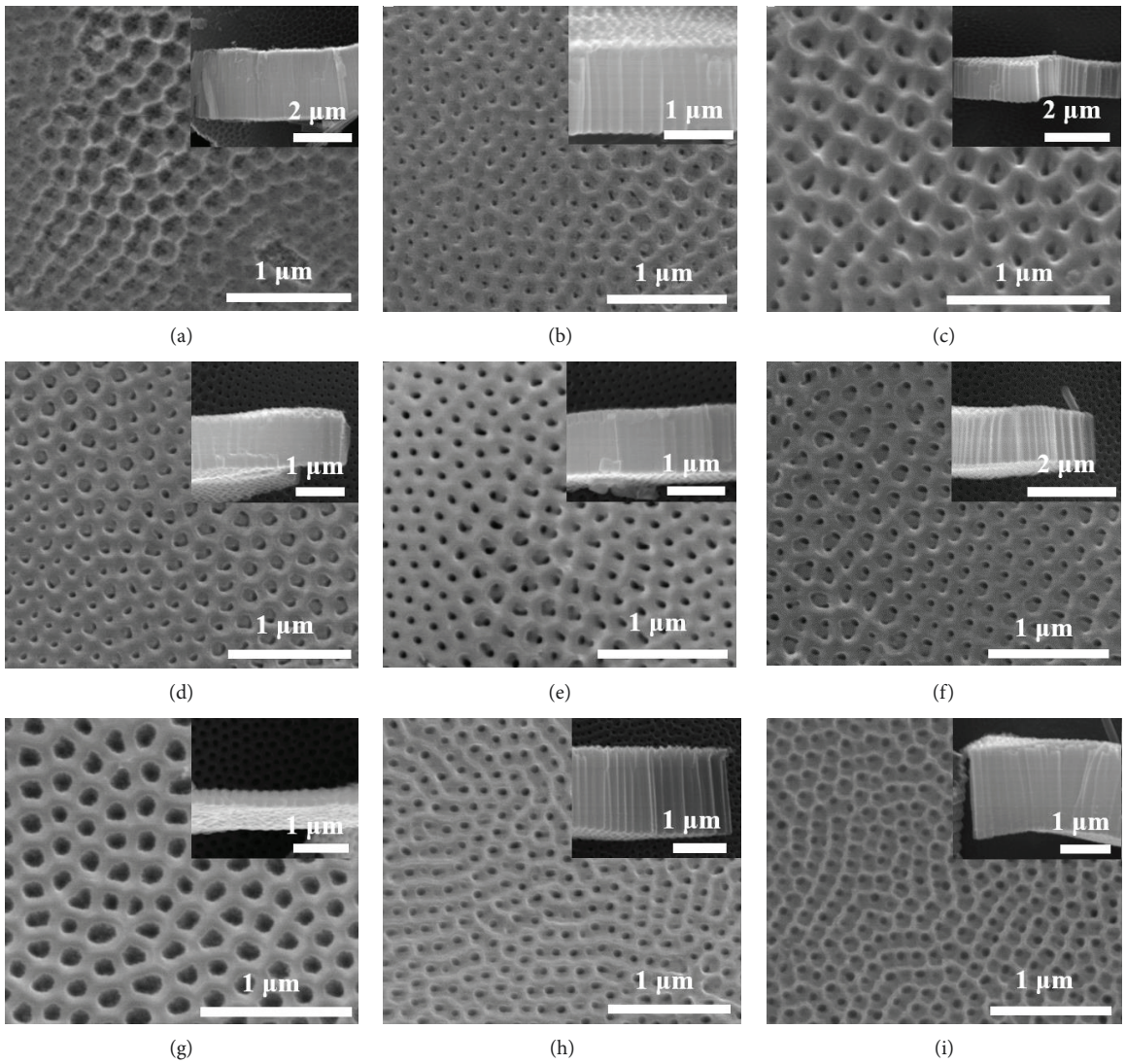

Figure 9: FE-SEM image of TiO_2 nanotube arrays with different voltage applying rate and dropping rate ((a) 0.1 V/s, immediately dropped, (b) 0.5 V/s, immediately dropped, (c) 1.0 V/s, immediately dropped, (d) 5.0 V/s, immediately dropped, (e) 10.0 V/s, immediately dropped, (f) 30.0 V/s, immediately dropped, (g) 60.0 V/s, immediately dropped, (h) 1.0 V/s, 1.0 V/s, and (i) 1.0 V/s, 0.1 V/s).

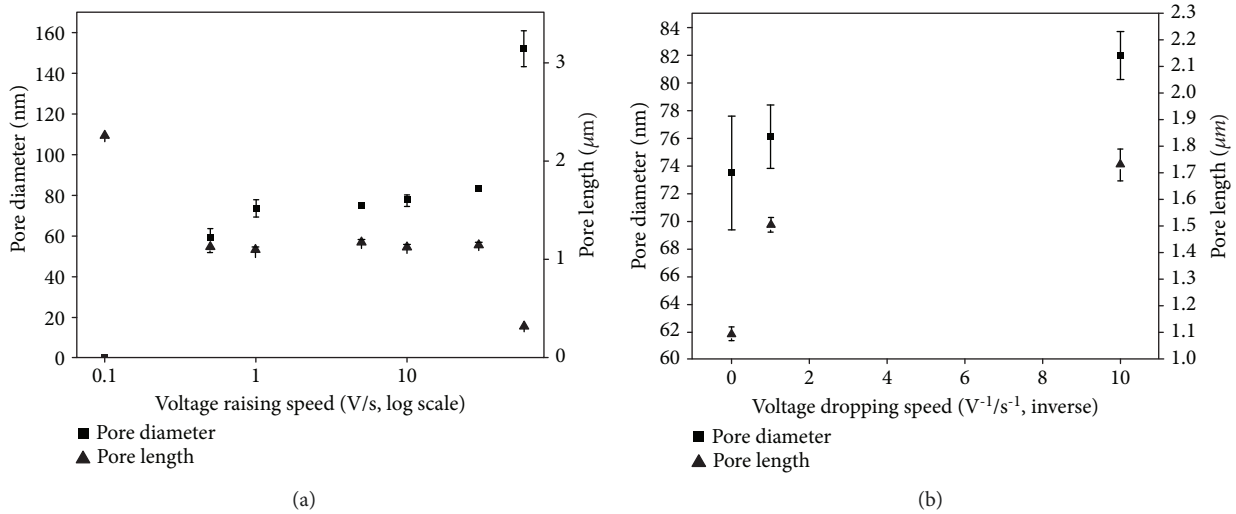

Figure 10: Pore diameter and pore length of TiO_2 nanotube arrays with different voltage applying rate and dropping rate.

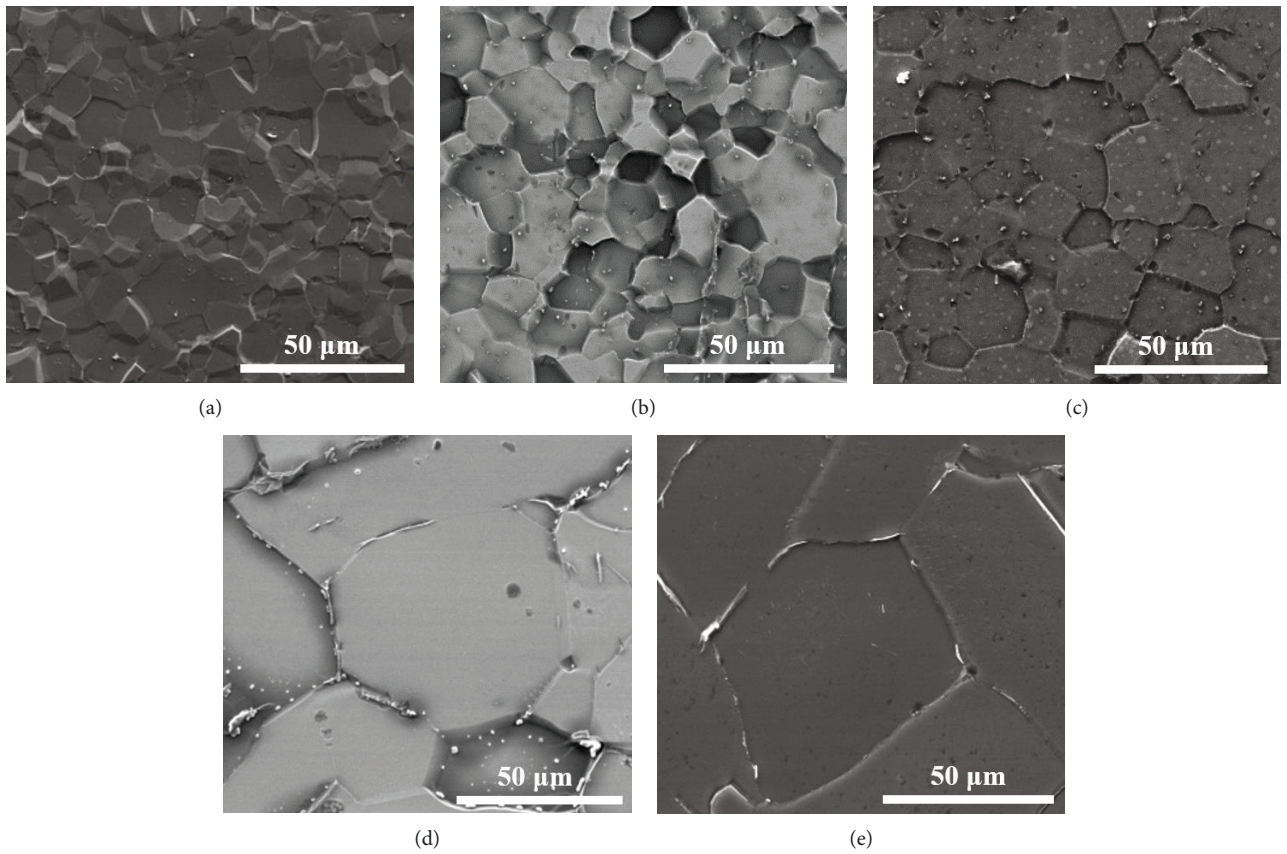

Figure 11: FE-SEM image of titanium grain with different annealing temperature ((a) not annealed, (b) 500°C, (c) 800°C, (d) 950°C, and (e) 1100°C).

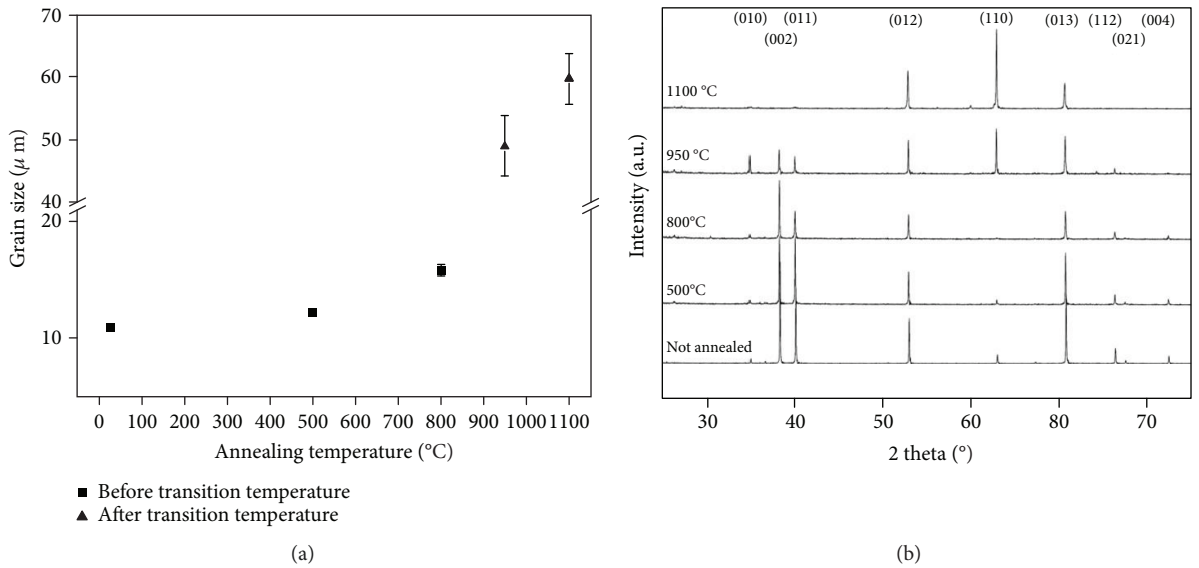

Figure 12: Grain size and crystal orientation of titanium foil with different annealing temperature.

glycol electrolyte with 0.5 wt% NH_4F and 8.2 vol% DI water. Figure 13 shows their FE-SEM image and microstructure changes. With the change of grain structure and orientation, there was no obvious change. They have about 110 nm of pore diameter and 3.3 μm of pore length.

4. Conclusions

To fabricate the various microstructured TiO_2 nanotube arrays by anodic oxidation, some process parameters such as applied voltage, process time, electrolyte temperature,

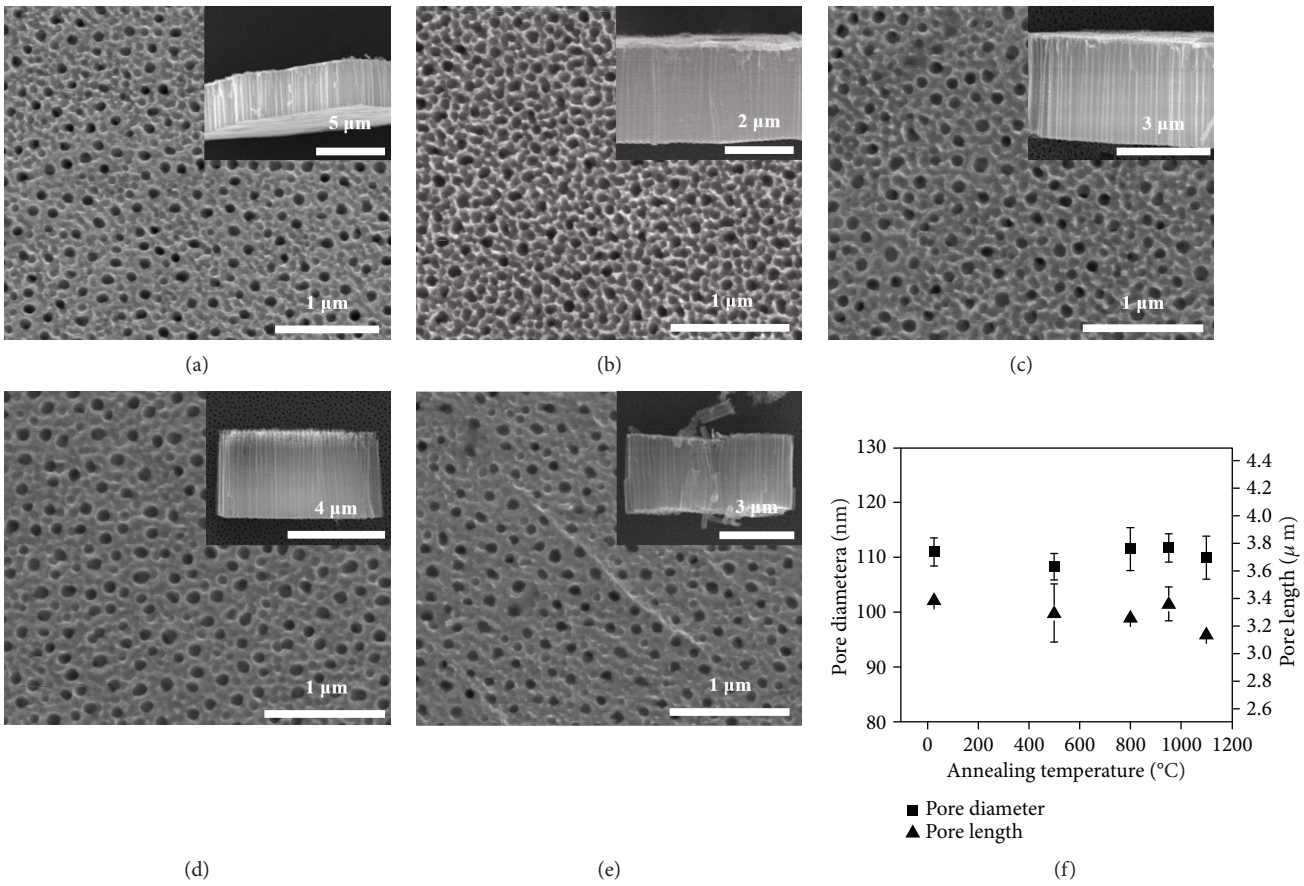

Figure 13: FE-SEM image and microstructure change of TiO_2 nanotube arrays fabricated on differently annealed titanium foil ((a) not annealed, (b) 500°C, (c) 800°C, (d) 950°C, and (e) 1100°C).

concentration of ammonium fluoride and DI water in ethylene glycol electrolyte, voltage applying and dropping rate, grain orientation, and size of titanium foil were controlled. With the increase of applied voltage, process time, temperature, and voltage dropping time, higher pore diameter and pore length were observed, and with the increase of ammonium fluoride and DI water concentration, higher pore diameter and lower pore length were observed. But with the increase of grain size and the change of crystal orientation of titanium, pore diameter and pore length were almost not changed. Typically, larger specific area with smaller pore diameter and longer pore length of TiO_2 nanotube arrays leads to a better performance of many devices, like photovoltaics, sensors, and photocatalysts. This growth tendency of TiO_2 nanotube arrays is should be considered before they used in many applications, and if optimal structure for each application was fabricated and used, they will show better performance.

Data Availability

The data used to support the findings of this study are included within the article.

Conflicts of Interest

There is no conflict of interest regarding the publication of this paper.

Acknowledgments

This research was financially supported by the Korea Institute of Energy Technology Evaluation and Planning (KETEP), the Ministry of Trade, Industry & Energy (MOTIE) (Grant No. 20181110200070), and the Local University Excellent Scientist Supporting Program through the National Research Foundation of Korea (Grant No. 2017R1D1A3B03036068).

References

[1] M. Grätzel, "Dye-sensitized solar cells," *Journal of Photochemistry and Photobiology C: Photochemistry Reviews*, vol. 4, no. 2, pp. 145–153, 2003.

[2] T.-H. Hwang, W.-T. Kim, and W.-Y. Choi, "Photoconversion of dye-sensitized solar cells with a 3D-structured photoelectrode consisting of both TiO_2 nanofibers and nanoparticles," *Journal of Electronic Materials*, vol. 45, no. 6, pp. 3195–3199, 2016.

[3] A. Hegazy, N. Kinadjian, B. Sadeghimakki, S. Sivoththaman, N. K. Allam, and E. Prouzet, "TiO_2 nanoparticles optimized for photoanodes tested in large area dye-sensitized solar cells (DSSC)," *Solar Energy Materials and Solar Cells*, vol. 153, pp. 108–116, 2016.

[4] M. Grätzel, "The light and shade of perovskite solar cells," *Nature Materials*, vol. 13, no. 9, pp. 838–842, 2014.

[5] S. I. Seok, M. Grätzel, and N. G. Park, "Methodologies toward highly efficient perovskite solar cells," *Small*, vol. 14, no. 20, article 1704177, 2018.

[6] N. J. Jeon, J. H. Noh, W. S. Yang et al., "Compositional engineering of perovskite materials for high-performance solar cells," *Nature*, vol. 517, no. 7535, pp. 476–480, 2015.

[7] N. T. Nguyen, M. Altomare, J. Yoo, and P. Schmuki, "Efficient photocatalytic H_2 evolution: controlled dewetting–dealloying to fabricate site-selective high-activity nanoporous Au particles on highly ordered TiO_2 nanotube arrays," *Advanced Materials*, vol. 27, no. 20, pp. 3208–3215, 2015.

[8] W.-T. Kim, I.-H. Kim, and W.-Y. Choi, "Fabrication of TiO_2 nanotube arrays and their application to a gas sensor," *Journal of Nanoscience and Nanotechnology*, vol. 15, no. 10, pp. 8161–8165, 2015.

[9] J. Bai and B. Zhou, "Titanium dioxide nanomaterials for sensor applications," *Chemical Reviews*, vol. 114, no. 19, pp. 10131–10176, 2014.

[10] W. T. Kim, J. K. Lee, I. S. Jang, D. S. Choi, and W. Y. Choi, "Surface improvement of TiO_2 nanotube arrays for dental implant," *Applied Mechanics and Materials*, vol. 864, pp. 78–83, 2017.

[11] W.-E. Yang, M.-L. Hsu, M.-C. Lin, Z. H. Chen, L. K. Chen, and H. H. Huang, "Nano/submicron-scale TiO_2 network on titanium surface for dental implant application," *Journal of Alloys and Compounds*, vol. 479, no. 1-2, pp. 642–647, 2009.

[12] W.-T. Kim and W.-Y. Choi, "Optical interference of TiO_2 nanotube arrays for drug elution sensing," *Science of Advanced Materials*, vol. 10, no. 2, pp. 283–287, 2018.

[13] K.-S. Mun, S. D. Alvarez, W.-Y. Choi, and M. J. Sailor, "A stable, label-free optical interferometric biosensor based on TiO_2 nanotube arrays," *ACS Nano*, vol. 4, no. 4, pp. 2070–2076, 2010.

[14] W.-T. Kim and W.-Y. Choi, "Fabrication of TiO_2 photonic crystal by anodic oxidation and their optical sensing properties," *Sensors and Actuators A: Physical*, vol. 260, pp. 178–184, 2017.

[15] Q. Xiang, J. Yu, and M. Jaroniec, "Synergetic effect of MoS_2 and graphene as cocatalysts for enhanced photocatalytic H_2 production activity of TiO_2 nanoparticles," *Journal of the American Chemical Society*, vol. 134, no. 15, pp. 6575–6578, 2012.

[16] I.-D. Kim, A. Rothschild, B. H. Lee, D. Y. Kim, S. M. Jo, and H. L. Tuller, "Ultrasensitive chemiresistors based on electrospun TiO_2 nanofibers," *Nano Letters*, vol. 6, no. 9, pp. 2009–2013, 2006.

[17] E. Formo, E. Lee, D. Campbell, and Y. Xia, "Functionalization of electrospun TiO_2 nanofibers with Pt nanoparticles and nanowires for catalytic applications," *Nano Letters*, vol. 8, no. 2, pp. 668–672, 2008.

[18] D. Kowalski, D. Kim, and P. Schmuki, "TiO_2 nanotubes, nanochannels and mesosponge: self-organized formation and applications," *Nano Today*, vol. 8, no. 3, pp. 235–264, 2013.

[19] L. V. Taveira, J. M. Macák, H. Tsuchiya, L. F. P. Dick, and P. Schmuki, "Initiation and growth of self-organized TiO_2 nanotubes anodically formed in $NH_4F/(NH_4)_2SO_4$ Electrolytes," *Journal of the Electrochemical Society*, vol. 152, no. 10, pp. B405–B410, 2005.

[20] J. Wang and Z. Lin, "Freestanding TiO_2 nanotube arrays with ultrahigh aspect ratio via electrochemical anodization," *Chemistry of Materials*, vol. 20, no. 4, pp. 1257–1261, 2008.

[21] R. Beranek, H. Hildebrand, and P. Schmuki, "Self-organized porous titanium oxide prepared in H_2SO_4/HF electrolytes," *Electrochemical and Solid-State Letters*, vol. 6, no. 3, pp. B12–B14, 2003.

[22] S. Berger, J. Faltenbacher, S. Bauer, and P. Schmuki, "Enhanced self-ordering of anodic ZrO_2 nanotubes in inorganic and organic electrolytes using two-step anodization," *physica status solidi (RRL) – Rapid Research Letters*, vol. 2, no. 3, pp. 102–104, 2008.

[23] N. K. Allam and C. A. Grimes, "Effect of cathode material on the morphology and photoelectrochemical properties of vertically oriented TiO_2 nanotube arrays," *Solar Energy Materials and Solar Cells*, vol. 92, no. 11, pp. 1468–1475, 2008.

[24] W.-Y. Choi, J. Chung, C.-H. Cho, and J.-O. Kim, "Fabrication and photocatalytic activity of a novel nanostructured TiO_2 metal membrane," *Desalination*, vol. 279, no. 1–3, pp. 359–366, 2011.

[25] J. M. Macak and P. Schmuki, "Anodic growth of self-organized anodic TiO_2 nanotubes in viscous electrolytes," *Electrochimica Acta*, vol. 52, no. 3, pp. 1258–1264, 2006.